J Mater Sci (2010) 45:5937–5949
DOI 10.1007/s10853-010-4679-x

Effect of dilute HF solutions on chemical, optical, and mechanical properties of soda–lime–silica glass

F. M. Ezz-Eldin · T. D. Abd-Elaziz · N. A. Elalaily

Received: 12 March 2010 / Accepted: 28 May 2010 / Published online: 22 June 2010

Abstract Commercially and laboratory prepared soda–lime–silica (SLS) glasses compositions were investigated for corrosion behavior toward varying dilute HF solutions. The corrosion is found to be low in 0.05 M HF solution and relatively high with 0.5 M HF. Infrared reflectance studies were measured to monitor the surface changes after etching process. The corrosion data are explained on the basis of selectivity of HF toward the bridging and nonbridging oxygens. Optical transmittance, impact toughness, and density were measured after corrosion; the data are used to verify the suggested corrosion mechanism. Significant changes were reached on the remeasurement of previous collective studied properties when the commercial glass was irradiated.

Introduction

Glass is generally considered to be a relatively stable and quite strong material but when it comes in contact with either liquid or water vapor it is vulnerable to decay [1]. The kinetics of cation leaching from silicate glasses are controlled by the extent and rate of reactions between aqueous solutions and the glass. In diluted aqueous solutions the early stage of alkali leaching is controlled by ion exchange, whereas the later stages of corrosion are controlled by network hydrolysis and dissolution [2]. The corrosion of a glass by acidic solutions is accepted to be governed by two processes [1–3]: (1) The leaching process which involves the introduction of H^+ ions (or H_3O^+) from acid solution, and the liberation of the alkali ions such as Na^+ ions or alkaline divalent ions from the glass surface into the solution, and followed by the dissolution of the silicate network via the hydrolysis of siloxane bonds. (2) The process of direct attack (etching process) is a process whereby breakdown of the silica structure and total glass dissolution occur [3].

The dissolution of silicate glass in hydrofluoric acid solution results in the formation of the stable hexafluorosilicate $(SiF_6)^{2-}$ anion [4–6].

The overall reaction is

$$SiO_2 + 6HF \rightarrow (SiF_6)^{2-} + 2H_2O + 2H^+ \quad (1)$$

This equation is a simplification of the reactions occurring during the heterogeneous SiO_2 dissolution by HF solution. Vitreous (as well as crystalline) SiO_2 consists of tetragonal SiO_4 units connected at all four corners with four other SiO_4 units by covalent $\equiv$Si–O–Si$\equiv$ (siloxane) bonds.

The mechanism of the reaction of hydrofluoric acid with silicate glass depends on the ionization process of the acid, which is expressed as follows:

$$HF \rightarrow H^+ + F^- \quad {}^{25}K_a = 6.7 \times 10^{-4} \text{mol/l} \quad (2)$$

where ${}^{25}K_a$ is the equilibrium constant at 25 °C.

In the presence of un-dissociated hydrofluoric acid, the fluoride ions react to form the bifluoride anion (HF_2^-) which is assumed to be responsible for the attack of the silica matrix [7, 8] and is expressed as follows:

$$HF + F^- \rightarrow HF_2^- \quad {}^{25}K = 3.96 \text{ mol/l} \quad (3)$$

It is accepted [1–3] that, throughout intermediate and long time, surface layers can be formed during the

F. M. Ezz-Eldin (✉) · N. A. Elalaily
National Center For Radiation Research and Technology, P.O. Box 29, 11765 Nasr-City, Cairo, Egypt
e-mail: fatthy1uk@yahoo.com

T. D. Abd-Elaziz
Faculty of Engineering, Industrial Chemistry Department, MSA University, 6th October City, Egypt

corrosion process. These layers are mainly formed from the precipitation of insoluble compounds near or within the leaching glass surface. The role of this layer depends on the properties of the layer, e.g., porosity, composition, and conditions of attack. Accordingly, such layer can have little or no effect on glass leaching or can provide an important protective barrier, which can reduce the rate of glass corrosion with time. This means that the precipitated layer has the potential of affecting further glass corrosion. The leached glass components must then pass through this outermost precipitated layer before being penetrated to solution [9, 10].

One of the important factors affecting the corrosion process is the ratio of surface area of the glass to the volume of the corroding solution, whereas the quantity of materials extracted from a silicate glass varies with this ratio. Paul [11] noticed that, the quantity of alkali and silica extracted increases as the glass surface area to the volume of the leaching solution increases.

Robert et al. [12] noticed in their IR spectral studies on silicate glasses that the OH groups are usually bonded to silicon, but recent NMR findings give evidence that additionally free OH^- ions are linked to Mg and Ca in alkaline earth silicates [13]. Also, Kohn et al. [14] have found that in aluminosilicate glasses, OH groups may also form bridges between two tetrahedral units.

Radiation effects are of important consideration because of the potential influence on glass corrosion stability [15]. Modification of the structure of simple glasses such as silica under external irradiation has been studied [16, 17]. Radiation damage to the solid glass results in bond damage and atomic displacements. This type of damage has been shown to increase the release rates of glass constituents up to four-fold during subsequent corrosion tests [18, 19].

The main objective of this study is to investigate the effect of two parameters, namely, degradation caused by intervals immersion time of HF solution with varying acid concentration on the etching behavior of commercial and simulated soda–lime–silica (SLS) glass under laboratory conditions. The aim is extended to study the effect of HF attacks on three of the most important properties of glass, namely, surface morphology, transmission, and mechanical. Also, in this study we report on the effect that HF etching has on the irradiated commercial glass samples after successive gamma-irradiation doses.

Experimental details

Glass preparation

The materials investigated in this study are based on a commercial SLS glass with the composition given in Table 1 as G1 of silicate glass system together with two others laboratory prepared simulated glasses of the same system: G2 and G3 which are also listed in Table 1. Highly purified silica was used as the essential network-former, sodium and calcium oxides were obtained from reagent grade corresponding carbonates. The weighed batch components were melted at a temperature of 1400 ± 10 °C in Pt crucibles, and allowed to homogenize (2 h). The glass was poured onto a stainless steel slab, and was immediately annealed at 450 ± 5 °C for 20 h. Glass samples were then removed, and were cut off in a size of 1 × 2 × 0.2 cm. Samples were cleaned by washing with few mL of alcohol followed by deionized water, then left in an autoclave at 100 °C for 1 h before any further exposure.

Etching procedures

Different leaching conditions have been used for the three studied of glasses (HF concentrations, immersion time, temperatures, and irradiation).

The procedure adopted of static etching experiments can be summarized as follows:

1. The glass coupons [1 × 1 × 0.2 cm] from the commercial (G1) and prepared (G2 and G3) SLS samples were cut, and their surfaces were carefully polished up to 3 μm grid. Glass specimens were kept in a dried atmosphere to avoid moisture pollution before testing.
2. The inlet solutions (0.05 or 0.5 M HF) used in this study comprised deionized water plus reagent grade of HF acid. The test duration ranged from 1 up to 25 days at room temperature (~25 °C) and, at different temperatures (40, 60, 80, and 100 °C) from 5 up to 25 h.
3. The glass coupons were accurately weighed on a Sartorius analytical balance with accuracy of ±0.1 mg, placed horizontally in a 200 mL polyethylene BD Falcon™ Conical Tube with Flip Top Cap, which allow the etchant solution (100 mL) to completely

Table 1 Chemical compositions of commercial and simulated (SLS) glasses (wt.%)

Glass number	SiO_2 %	Na_2O %	CaO %	MgO %	Al_2O_3%	K_2O %	SO_3 %	Fe_2O_3 %
G1	71.9	14.2	8.6	4	0.7	0.04	0.3	0.085
G2	72	18	10					
G3	70	20	10					

cover the whole glass surfaces of the specimen, and then the tube is tightly closed.

4. The glass samples were left in the acid for 5, 10, 15, 20, and 25 days at 25 ± 1°C. Other Imhoff cones containing glass samples of the same compositions were placed in a water bath at 40, 60, 80, and 100 °C (±2 °C) for 5, 10, 15, 20, and 25 h.
5. The glass specimens after the fixed times were washed in de-ionized water and left to dry in air after immersion in each specific acid solution and then reweighed after each time interval. The measurements for weight loss were carried out in triplicate. During etching test, the temperature and humidity rate in the laboratory were nearly constants: ~25 ± 1 °C and 43 ± 5% RH, respectively.
   - As the etching is affected by surface area, so the relationship between the geometric surface area of the glass samples and the volume of the solutions was maintained as 0.021 cm^{-1} in all cases for comparison and to avoid effects due to volumetric differences [20].
6. The Na^{+} ions released in the etchant solution for irradiated G1 glass was determined by using atomic absorption technique (Model, Perkin Elmer, Zeeman 5000)

FTIR spectroscopy measurements

FTIR specular reflectance spectra were measured with Jasco FT/IR-430, Japan at the range 4000–400 cm^{-1}. This technique was used to monitor the chemical surface changes caused by the HF etching treatments. Analysis was performed before and after all treatments for all the glasses. The measurements were done using a spectrometer equipped with a liquid nitrogen-cooled mercury-cadmium telluride detector and a variable angle specular reflectance accessory set to 84° at room temperature with resolution 2 cm^{-1}. Doubly polished glass plates with thicknesses in the range of 0.3–0.7 (±0.02) mm were prepared for FTIR spectroscopy. Each spectrum was taken as an average of 10 scans collected over the frequency range of 1300–400 cm^{-1} with a resolution of 4 cm^{-1}.

SEM measurements

Photomicrographs of the etched and unetched SLS glass were performed using a JSM-5400 Scanning electron microscope (SEM). Before and after the etching experiments the glass samples were rinsing in deionized water followed by a final ethanol bath and drying. After etching, the analytical procedures were performed immediately to avoid uncontrolled alteration of the glass surfaces.

Optical transmittance measurements

Absorption spectra in the UV-Vis range were obtained by means of a double beam spectrophotometer (type JASCO Corp., v-570, Rel-00 Japan) covering the range 200–1100 nm. For absorption measurements the spectral bandwidth was kept to 1 nm.

Impact toughness and density measurements

Samples having dimensions of 75 mm length, 10 mm width, and 10 mm thickness were prepared for the fracture toughness test. Impact test was carried out on a pendulum type Charpy's instrument (model PSW4Joule). The specimens had a mid span notch of 2 mm depth and were fractured at room temperature. The amount of energy absorbed up to fracture of the specimen was recorded in joules, according to the following equation: $a_k = A_k/b{\cdot}h_k$ where: a_k impact toughness, A_k absorbed impact energy in joules, b, and h_k are the width and thickness of the test specimen in the notch center in cm, respectively. For each test, ten tests were performed. The average values for ten tests of the impact toughness were then determined.

The density values which are the average of three measurements were measured by applying the Archimedes method using xylene as immersion liquid with an estimated error ±0.0001 gm/cm^3.

Gamma-irradiation facility

A ^{60}Co gamma cell (2000 Ci) was used as a gamma-ray source with a dose rate of 1.5 Gy/s at a temperature of 30°C. The investigated glass samples were subjected to the same gamma dose every time using a Fricke dosimeter, the absorbed dose in water was utilized in terms of dose in glass. No cavity theory correction was made. The given doses are 40 and 80 KGy.

Results

Etching results

The relationship between the immersion time (days or hours) and the etching weight loss per unit area (g/cm^2) at different temperatures is emphasized in Figs. 1, 2, and 3, where the weight losses (g/cm^2) from specimens immersed for varying times in solutions with two different concentrations of HF (0.05 and 0.5 M) are reported. It can be noticed that at low concentrations of HF, the amount of corrosion weight loss is small, but when the HF solution concentration is increased to 0.5 M, the dissolution of glass is rapid and extensive.

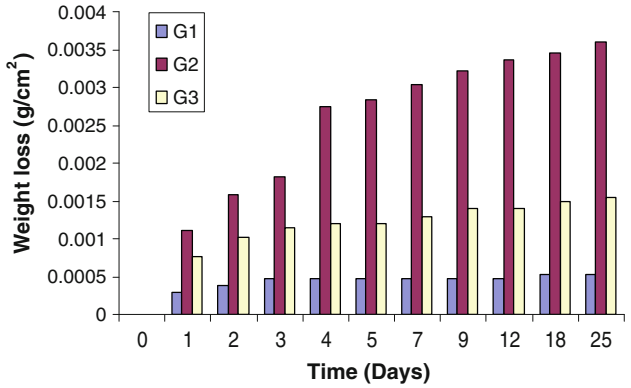

Fig. 1 Corrosion behavior of G1, G2, and G3 glasses immersed in 0.05 N HF at RT

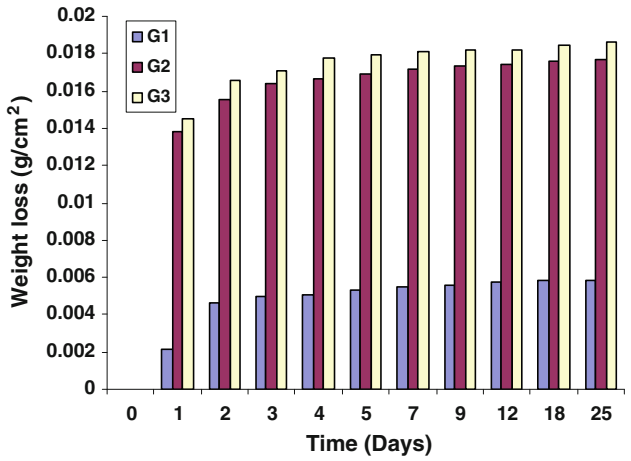

Fig. 2 Corrosion behavior of G1, G2, and G3 glasses immersed in 0.5 N HF at RT

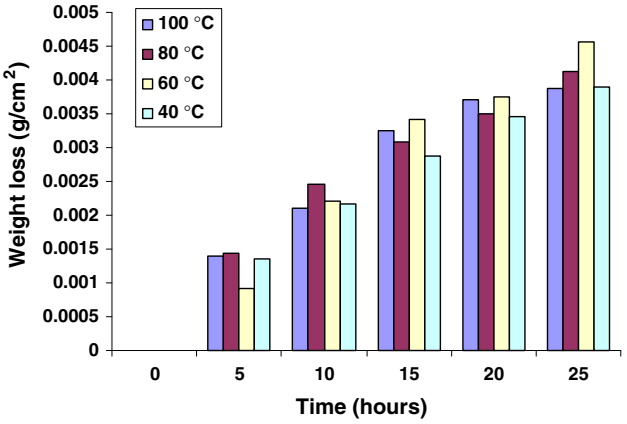

Fig. 3 Effect of different temperatures on the corrosion behavior of G1 glass immersed in 0.5N HF at RT

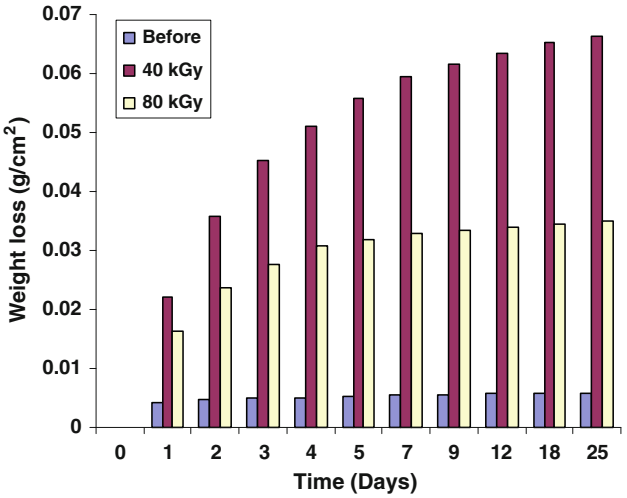

Fig. 4 Effect of different irradiation doses on the corrosion behavior of G1 glass immersed in 0.5 N HF at RT

The results in Figs. 1 and 2 show the effect of increasing Na_2O content in simulated glasses G2 and G3 on the corrosion behavior at either 0.05 or 0.5 M HF at room temperature. From these figures, it is obvious that as the amount of Na_2O increases(G3), the corrosion increases, while the corrosion of glass G1 is very low as compared with that observed with the other two simulated glasses. The results also reveal that the large amount of corrosion weight loss rapidly increases at the early periods of immersion followed by a decrease in the corrosion rate afterward, which is accompanied by some sort of constancy.

Figure 3 shows that the weight loss(g/cm^2) of glass G1 immersed in 0.5 M HF slightly increases relative to raising the etching solution temperatures (40, 60, 80, and 100 °C), but after immersion for 15 h and at 60 °C there is an increase in weight loss which exceeds that recorded either at 80 or 100 °C**.**

The results (Fig. 4) reveal that, when the glass G1 is irradiated at 40 kGy and immersed in 0.5 M HF, a dramatic increase occurs in its corrosion, followed by a decrease in the amount of corrosion at high irradiation dose (80 KGy) but its corrosion still higher than the unirradiated glass sample. Generally, from Figs. 1, 2, 3, and 4 we can observe that there is a slowing rate in the weight loss with increasing the immersion time.

The amounts of released Na^+ ions in the etchant solution for the irradiated and unirradiated glass G1 and immersed in 0.5 M HF for 25 days at RT are illustrated in Fig. 5. The data show that there is an increase in the amount of released Na^+ with increasing either immersion time or irradiation dose.

Fourier transform infrared (FTIR) spectroscopy measurements

The FTIR reflectance spectra of the corroded commercial (SLS) samples are shown in Figs. 6, 7, 8, and 9. The IR spectra are divided into two separate parts to avoid

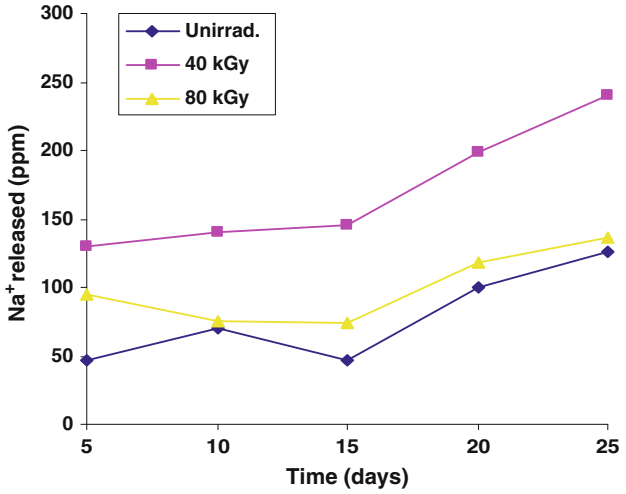

Fig. 5 Released Na_2O (ppm) for the irradiated and unirradiated glass (G1) after been immersed in 0.5 N HF as a function of immersion time at RT

confusion resulting from the complex nature of the IR spectra. It is evident that, the effect of changing HF acid concentration on the etching solution is not affecting the mechanism of corrosion, but only changes the amount of corrosion. Each IR spectrum is a snapshot of corrosion occurring after 25 days. The main peaks in Fig. 6 are observed at 1100, 750, and 470 cm^{-1}; the sharpness of the peak at 470 cm^{-1} increases with the decrease of HF concentration. However in Fig. 7, the percentage of reflectance is observed to increase as the etching time increases. The presentation of the IR bands of corroded glass (G1) at different temperatures (60, 80, and 100 °C) is indicated in Fig. 8. The results show that the main characteristic bands almost still have the same wavelength. The IR spectra also show an increase of the reflectance% with the increase of temperature of corrosion. The FTIR spectra of glass irradiated (40 kGy) before being immersed in 0.5 M HF solutions are shown in Fig. 9 which reveals that the reflectance% is remarkably increased for the irradiated glass.

Transmission

Optical transmissions of the immersed and non-immersed glass windows have been used to measure the optical properties of the glasses to improve the understanding and interrelation between the transmission and corrosion behavior. The average transmittance of glass G1 varies from 88 to 82% in the wavelength region of 350–700 nm. It is evident from the spectrum (Fig. 11) that the *T*% of glass changes after etching. However, the *T*% is swinging between increasing (5 days) and decreasing (10–25 days) accompanied with a shift toward longer wavelength (Fig. 12).

It can be seen from the transmittance curves of the glasses investigated that the short-wavelength cutoff of the broad band (390–590 nm) is shifted to shorter wavelength side if the HF concentration increases and to longer wavelength side if the immersion time increases. It is obvious from inspection of Fig. 13 that the effect of etching on the irradiated glass (G1) leads to a decrease of T% (40 kGy) in comparison with the unirradiated glass. But after higher irradiation dose 80 kGy, the transmission increases in the wavelength range 350–700 nm with a shift to lower wavelength as compared to the glass irradiated with a lower dose.

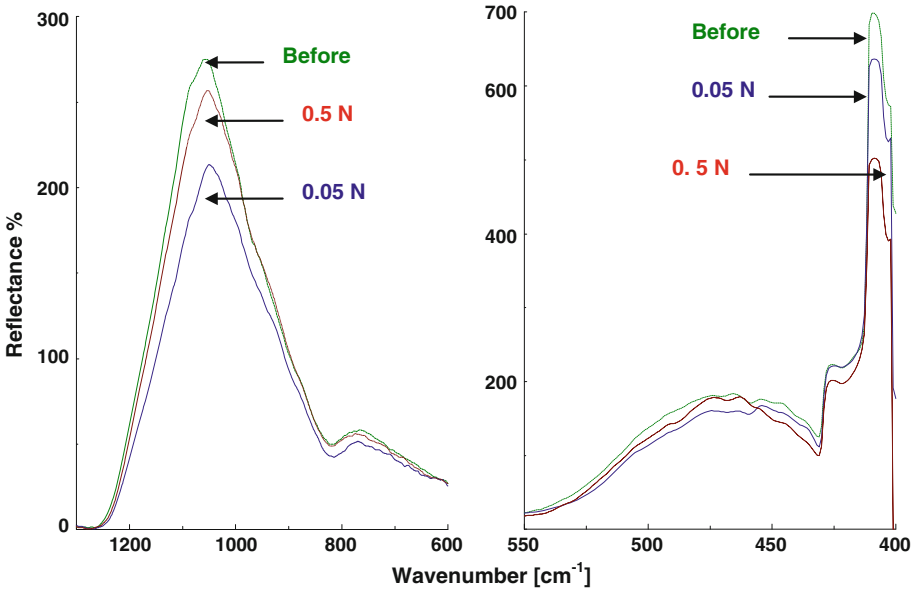

Fig. 6 Infrared reflectance spectra for G1 glass after been immersed in different HF concentrations for 25 days at RT

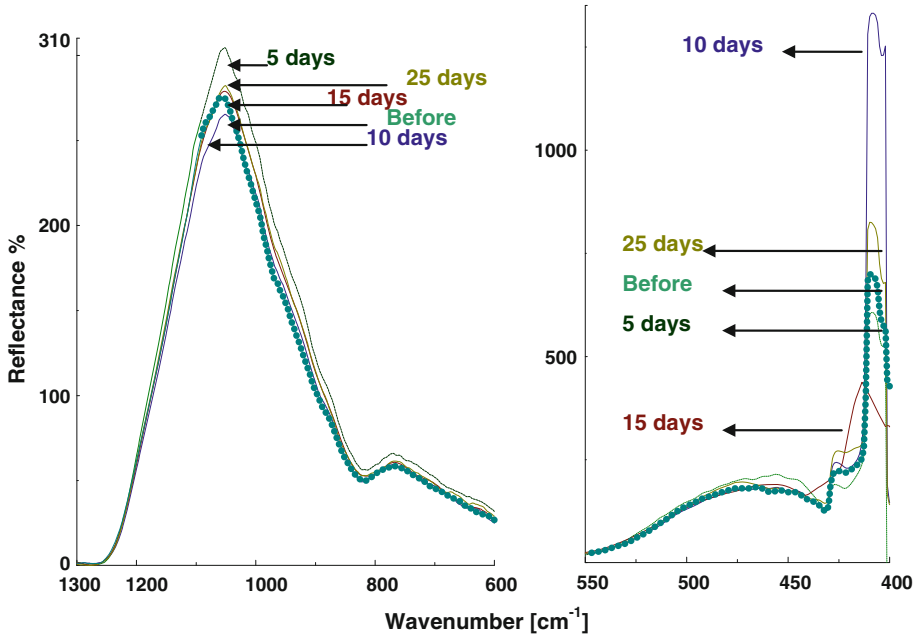

Fig. 7 Infrared reflectance spectra for G1 glass after been immersed in 0.5 N HF at different immersion periods at RT

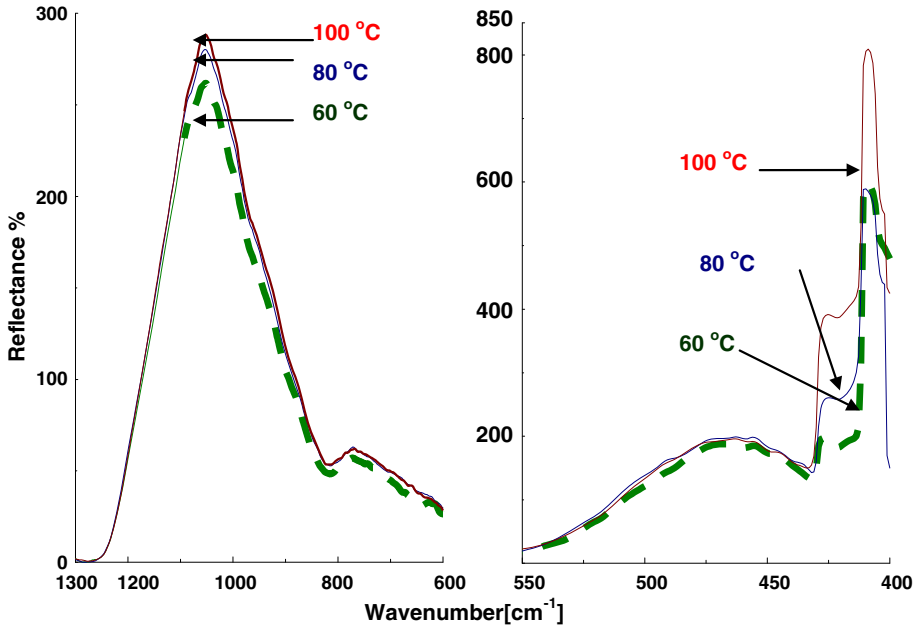

Fig. 8 Effect of different temperatures on the infrared reflectance spectra for G1 glass after been immersed in 0.5 N HF for 25 h

Impact toughness

The results of impact toughness for the SLS glass samples immersed in different concentration of HF acid solutions (0.05–0.5 M) are presented in Fig. 14. According to these data, it is evident that the impact toughness decreases gradually with increasing HF concentration, while it increases with increasing immersion time up to 15 days and then slightly decreases at 25 days. The same trend is observed when the temperature of immersion solutions is raised (Fig. 15).

Density

It is evident from Fig. 16 that the density values decrease as the corrosion increases, i.e., with increasing of either concentration of the solution or the immersion time until certain time where it results in an increase in density for the glass immersed in 0.05 M HF.

An improvement in both impact toughness and density for the unetched glass sample is observed after been irradiated (40 and 80 kGy) as shown in Figs. 17 and 18. Generally, etching for the irradiated or unirradiated glass

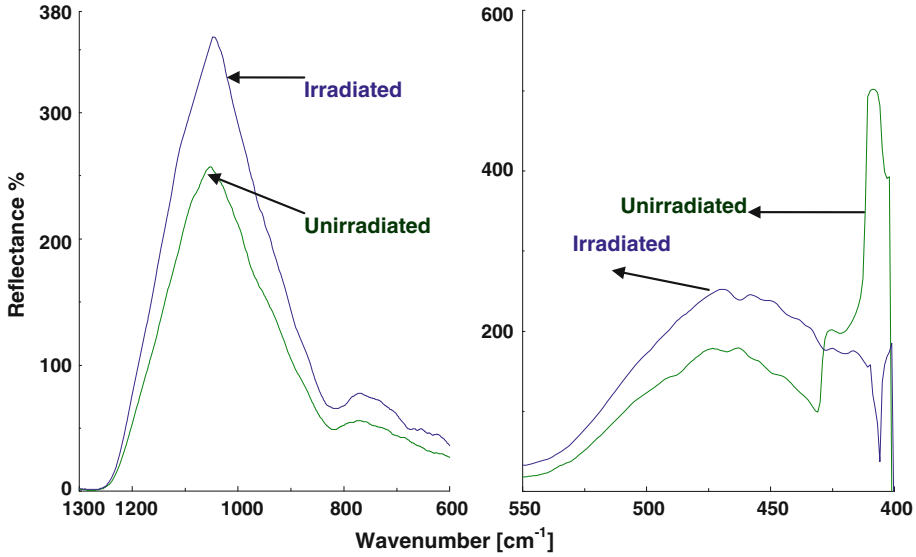

Fig. 9 Infrared reflectance spectra for the irradiated (40 kGy) glass G1 and immersed in 0.5 N HF for 25 days at RT

(G1) leads to the detoriation of impact toughness, but improves its density.

Discussion

It is accepted that [21] the etching of commercial SLS glass surface by dilute HF aqueous solution can be used during optical fabrication to convert glass surface damage into surface roughness thereby reducing the time required to produce polished surfaces that are free of surface damage**.**

Interpretation of the etching measurements

One of the most important properties of glass is its chemical durability and any dissolution on its surface may lead to a rough surface of the glass altering therefore its mechanical and optical properties [22]. The dissolution kinetics depend on many experimental parameters such as surface area, time, and temperature of the surrounding medium, while the thermodynamic contribution is a function of the composition of glass and its structure [23].

The increase of the amount of corrosion with the increase of the HF concentration for glass G1 is assumed to be due to the selectivity of HF solutions. The explanation of the selectivity has been attributed to the performance or the suitability of dilute HF for nonbridging oxygen (NBO) atoms which do not require a slow eliminate or addition step and hence reacts faster than bridging oxygen [24]. Concentrated HF solutions on the other hand, attack both bridging and nonbridging oxygens. This means that the lower the etch rate, the more selective etching takes place.

The results show that commercial SLS glass (G1) is highly durable compared to the laboratory prepared simulated glass (G2 and G3) according to Figs. 1 and 2. This may attributed partly to the presence of Mg^{2+} ions which results in the formation of MgF_2 during the corrosion process, which has a strong bond and protects Si–Si bond from being severely attacked by F^- ions. In addition, the number of imperfections in the commercial SLS glass is rare compared to those in prepared SLS glasses. On the other hand, we cannot ignore the role of sodium oxide content in glasses G2 and G3 compared to G1 which is the main factor in the observed detoriation of the durability for the glass G2 and G3.

The slight decrease in the glass durability at 80 and 100°C (Fig. 3) can be interpreted by the fast formation and deposition of the protective layers at high temperatures in the glass surface from $=SiF_2$, $SiHF_3$ and MgF_2, which seem to prevent more attacking of the solution.

The observed slowing rate in weight loss (g/cm^2) for all etching measurements when the immersion time is increased, can be attributed to be due to the continuous or simultaneous diminishing concentration of the HF acid related to the formation of hexafluorosilicic acid according to reaction (1).

The effect of gamma-irradiation on the corrosion behavior (Fig. 4) can be understood and realized by considering the effect of irradiation on the glass itself. Gamma-irradiation can cause changes in the electronic distribution within the glasses. Electrons freed by irradiation become trapped at impurity atoms or at imperfections and lead to the formation of radiation-induced defects. Such generated induced defects are expected to change the rate of corrosion weight loss. Moreover, it is assumed that gamma-irradiation causes the enhancement of the penetration of proton or hydronium ions from solution to the formed induced defects [25, 26]. There is also a possibility

that at high irradiation dose, a sequence of bond-breaking reactions may cause large molecular islands to dissolve from the glass surface and all these assumptions explain the observed corrosion results.

It is also believed that prolonged irradiation may produce groups of vacancies until a certain limit, after which defect saturation or annihilation process may occur [25–27]. In this case the weight loss due to corrosion is seen to decrease. This effect may be due to the occurrence of some sort of annihilation or rebonding processes in the glass lattice with prolonged irradiation.

The increase in amount of Na^+ ions released in the etchant solution (Fig. 5) either after irradiation or at long immersion time can be interpreted to be due to the presence of these Na^+ ions in the interstices between the silicate network. So, when the silicate bonds are broken due to irradiation and during the attack by HF solution, Na^+ ions become free to release in the solution.

Infrared spectra interpretation

The hydrous species generated during the corrosion process of glass by aqueous solutions are assumed to have different effects on the structure and properties of silicate glasses. The formation of OH groups results in depolymerization and weakening of the silicate network [14]. On the other hand, H_2O molecules play an important role in water diffusion and degassing of silicate melt [28]. It is possible to use the shift of the wave number location of the IRRS peaks to indicate the change in composition or type of groupings of the glass surface, independent of roughening or surface deposition.

The presence of OH groups and water molecules is usually monitored by infrared spectroscopy at higher wavenumbers (1600–4000 cm^{-1}). In this article, the IR spectrum within the range 400–1400 cm^{-1} is measured. Jin Cheng and Chormack [29] postulated that the variations in the absorption bands in the silicate glasses are attributed to several reasons; the first one is due to oxygen atom in the network structure Si–O–Si configuration; the second due to oxygen atoms in the intermediate, e.g., Si–O–Na configuration; and the third due to oxygen atom in neighborhood to a modifier, e.g., Si–O–Na^+, but there is an Si–OH stretching peak in the region of approximately 900–1000 cm^{-1} [9, 30]. This last peak can be considered as an indication of water in the glass structure and is typically associated with the SiO_4 in the glass surface.

Usually, Si–O–Si bond rocking is observed in silicate glasses within 410–490 cm^{-1} range. Therefore, the band at $\sim$470 cm^{-1} can be ascribed to the Si–O–Si bending mode.

The region where significant Si–O stretching (S) $\sim$1000–1100 cm^{-1} and silicon oxygen-alkali stretching (NS) peak at $\sim$960–1000 cm^{-1} overlap is called the coupled region [31]. Exposure of the glass surface to a chemical environment alters the relative concentration of both the silica and alkali species due to preferential leaching of alkali ions, and then produces a change in the infrared reflection spectra which is referred to the decoupling of the S and NS peaks due to selective alkali leaching [32]. The corrosion in low concentration of HF (0.05 M) solution may be responsible for the remarkable decrease in the percentage reflectance (Fig. 6) and the shift for the peak at $\sim$1059–1050 cm^{-1} which is mainly due to the dissolution of silicon ions.

According to Lynch [33], this peak may be a combination of Si–O-Si and Si–OH groups at the surface which are changed to Si–F after corrosion. Increasing the acid concentration to (0.5 M), the wave number slowly shifts toward the higher wave number ($\sim$1052 cm^{-1}) due to the formation of $=SiF_2$ and $SiHF_3$ in the glass surface [34]. Also, the reflectance% is observed to increase due to the dissolution of silicon and sodium ions in silicate matrix which are produced according to following equation:

$$\equiv Si{-}O{-}Na^+ + H_3O^+ \rightarrow \equiv Si{-}OH + Na^+ + H_2O \quad (4)$$

In addition, extensive surface reactions can lead to roughening of the surface due to the formation of either pits or surface deposits. The extent of surface roughening can be measured by the decrease in intensity of the IRRS peak. If a decrease in IRRS peak intensity occurs without a significant change in wave number, it indicates that surface roughening is occurring [35].

Moreover, Clark et al. [3] have found that, the increase in wave number within the IR spectra is due to the selective leaching of alkali and development of a SiO_2-rich film on the glass surface. The wave number shifts are correlated with the composition data yielding the time dependence of the surface alkali content. As the reaction time increases, the alkali content of the glass surface changes and consequently decreasing the amount of sodium content in the composition of the glass surface. In this study, it is evident (Fig. 7) that since HF solution attacks the silicon ions, the amount of silica increases at the first time interval (5 days) due to the formation of SiF_4 layer in the glass surface before its dissolution, while, after 10 days it shows a decrease in the reflectance%. But, increasing time intervals to 15 days there is an increase in the reflectance% due to the release of both silicon and sodium ions which are housed in the voids of the silicate network. Further increase in the etching time (25 days) does not show a noticed change in the glass surface which can be explained by assuming the formation of gel layer on the glass surface retarding or preventing any further attack of HF solution.

According to Fig. 8, the reflectance% increases for all the main peaks relatively with rising temperature which means that the intensities of the main peaks at Si–O–Si stretching band at $\sim 1050\ cm^{-1}$, Si–O– stretching band at $\sim 750\ cm^{-1}$, and Si–O–Si bending band at $\sim 470\ cm^{-1}$ increase. According to previous etching interpretation, it is assumed that the corrosion decreases for glass etched at 100°C due to the possible formation of $=SiF_2$ and $SiHF_3$ layers in the glass surface which in turn increases the amount of Si–O vibrational groups in the IRRS results which reflect the surface structure.

The effect of etching on the irradiated SLS glass surface (40 kGy) indicates an increase in the reflectance% (Fig. 9). This is may be due to the decrease in concentration of nonbridging oxygens (NBO's) after irradiation. Another postulation can be introduced that liberated electrons and positive holes during irradiation reacts with NBO's sites creating induced defects, which obliges the silanol groups in corroded glass to react with each other to form new Si–O–Si bonds via reaction (5)

$$\equiv Si{-}OH + HO{-}Si \equiv \rightarrow \equiv Si{-}O{-}Si \equiv + H_2O \quad (5)$$

If reaction (5) is to go to completion, the products would be amorphous or gelatinous silica and water [36].

Interpretation of SEM measurements

The produced damages of the surfaces of the etched SLS glass samples are displayed on SEM images (Fig. 10). They show surfaces condition before and after etching treatment in 0.5 M HF for different interval times (5, 10, 15, and 25 h) at ~ 60°C. This type of SLS glass is assumed to develop corrosion patterns which appear rather faint at the first time of etching. Also, it is observed that there is a progress in the damage which occurs in the glass surface with the increase of etching time. Also, at the last two photos (d and e), it is shown that a gel layer is formed containing flackes while the parts free from the gel layer shows cracks in the glass surface. These damages are assumed to be due to the reformation of silicate groupings and transformation from $Si–O–Na^+$ to Si–OH, and Si–O–Si to $\equiv Si–F$, $=Si–F_2$ and $–Si–F_3$, through different possible chemical reactions.

Interpretation of the optical transmittance

All transmittance results are summarized in Figs. 11 and 12 showing a swinging between increasing and decreasing of transmittance percent. The increase in transmittance either with increasing HF concentration or at the early immersion times may be due to liberation of OH from silanol groups according to the following equation [37].

$$\equiv Si{-}OH + HF \rightarrow \equiv Si{-}F + H_2O \quad (6)$$

The observed decrease in the transmittance% may be explained by assuming that, during the etching process, the microcracks which are already present on the glass surface are believed to be widen and opened and thus leading to the reflection and the diffusion of light inside the microcracks (on the flanks of microcracks). This confirms the deduction that the opening up of the microcracks increases with the increase of either HF concentration or immersion time leading to a reduction in transmittance. Another explanation can be put forward by assuming that this decrease can be expected in view of the increase in surface reflection with angle of incidence, as well as the longer path in the material. It is also important to observe that at high angles of incidence, the transmission of the glass decreases more at longer than at shorter wavelengths [38].

Upon irradiation, the optical results (Fig. 13) show degradation followed by improvement in the transmission edge between 350 and 500 nm, when the irradiated samples are etched. Thus, these variable changes of the transmission% could be correlated with the changes of induced occupation defects with charge carriers, creation of radiation defects in the cation and anion sublattice and the formation of optical centers (NBO hole centers) on clusters of these defects [25]. Also, if some of the Fe^{2+} ions are assumed to be oxidized to Fe^{3+} through photochemical reactions by irradiation process, one might expect a decrease in transmission at ~ 380 nm. Moreover, the observed shifts either toward the shorter or longer wavelength can be explained as follows: when the shift is toward the shorter wavelength side, thereby increasing the transmittance region, which enables more light to pass through the sample. Similarly, when the irradiation dose is increased, it leads to self-absorption (cutoff shifts to longer wavelength side) and hence the decrease in the transmission intensity [39].

Impact toughness and density data interpretation

In order to investigate the reason for the changes in the impact crack formation by etching, impact toughness was measured which is the one of the factors affecting the resistance of the formation of cracks. It is reported that the hardness of the glass surface decreases with increasing concentration of the silanol group (SiOH) [40]. Furthermore, it is also known that a hydrated layer with a large concentration of the silanol groups, which originates from an ion exchange reaction induced by adsorbed water, is formed on the glass surface [41]. The observed increase in impact toughness (Fig. 14) with increasing the immersion time (after 15 days) can be explained by the

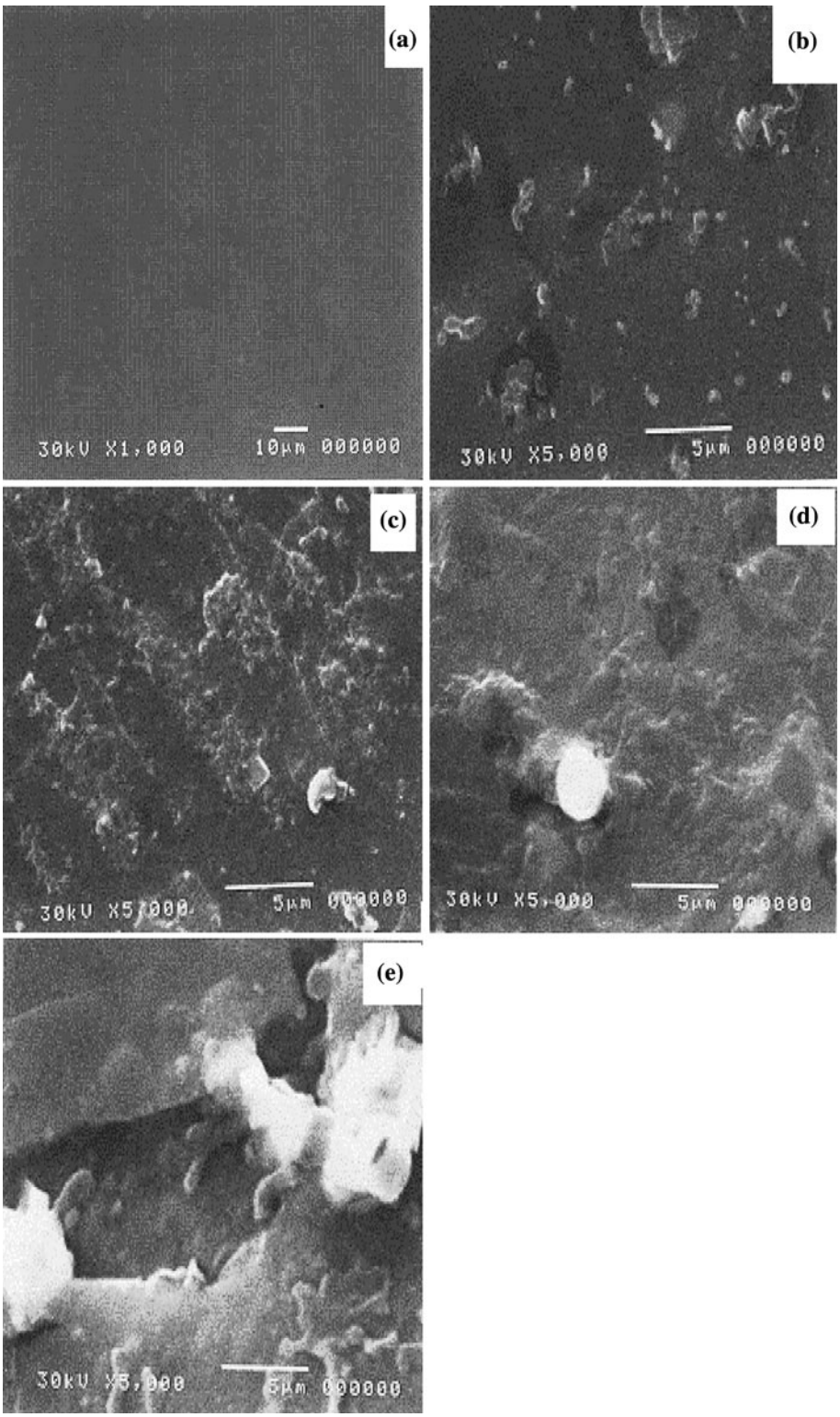

Fig. 10 Effect of different immersion times; **a** virgin, **b** 5, **c** 10, **d** 15, and **e** 25 h on the surface morphology of SLS glass immersed in 0.5NHF at 60°C

assumption that, when the HF solution attacks on the surface leading to the formation of the Si–OH links, but on the other side it leads to reinforcement of the Si–O links. The slight increase in impact toughness with elevating the solution temperature (Fig. 15) is due to the gradually removing of silanol groups and then rendering the glass surface more durable. However, the degradation in toughness with increasing immersion times is attributed to the progressive attack of solution on the whole surface, and particularly inside the microcracks, rendering them curved at both ends and consequently reduce the toughness.

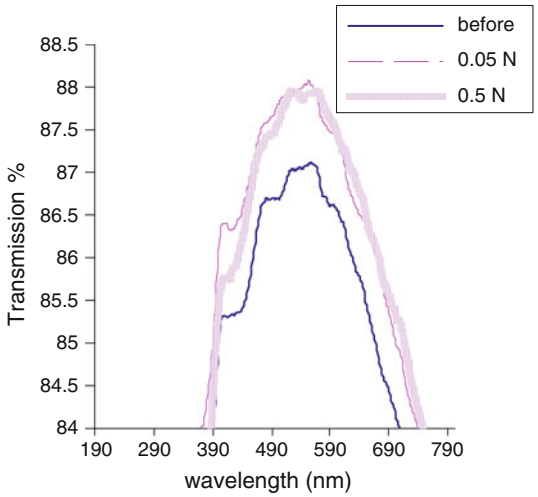

Fig. 11 Effect of different HF concentrations on the optical transmission of G1 glass after been immersed for 25 days at RT

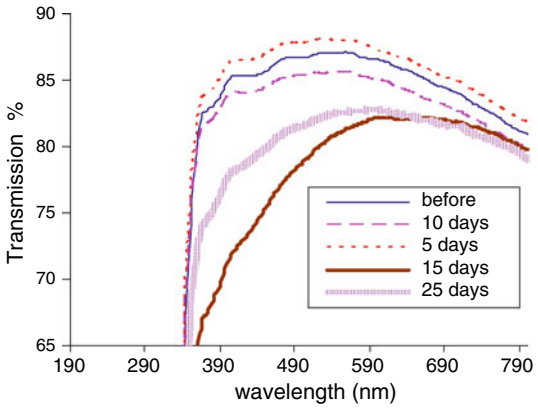

Fig. 12 Effect of different immersion times on the optical transmission of G1 glass immersed in 0.5 N HF at RT

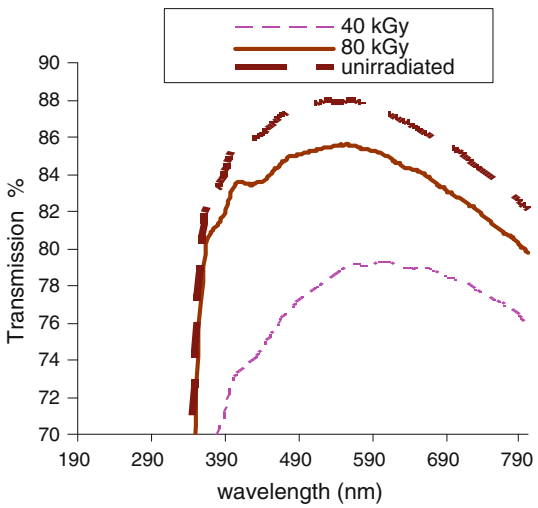

Fig. 13 Effect of different irradiation doses on the optical transmission of G1 glass immersed in 0.5 N HF at RT

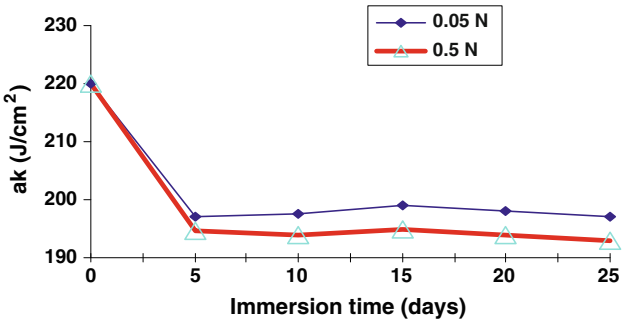

Fig. 14 Effect of different HF concentrations on the impact toughness of G1 glass after been immersed for 25 days at RT

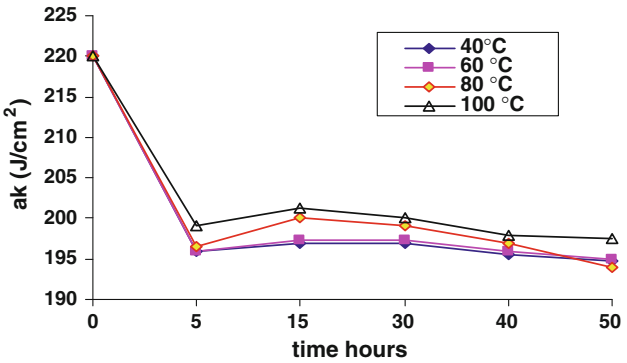

Fig. 15 Effect of different temperatures on the impact toughness of G1 glass after been immersed in 0.5 N HF

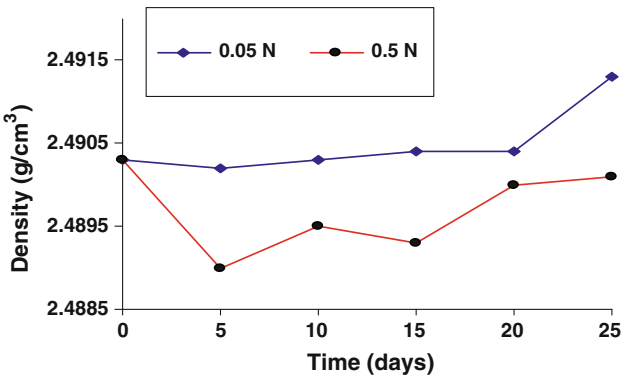

Fig. 16 Effect of different HF concentrations on the density of G1 glass after been immersed for 25 days at RT

A strong correlation was observed by Boenisch et al. [42] between the dissolution rates as a function of glass density, noting that increasing of SiO_2 content causes a decrease in glass density. In the present results (Fig. 16) it is observed that there is an increase in the glass density with increasing the immersion time, and this can be understood and explained as follows: long etching time leads to a progressive dissolution of surface Si ions causing increase in density. Also, the experimental results show a

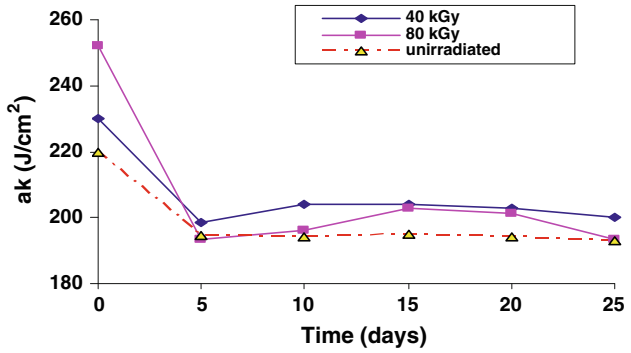

Fig. 17 Effect of different irradiation doses on the impact toughness of G1 glass after been immersed in 0.5 N HF at RT

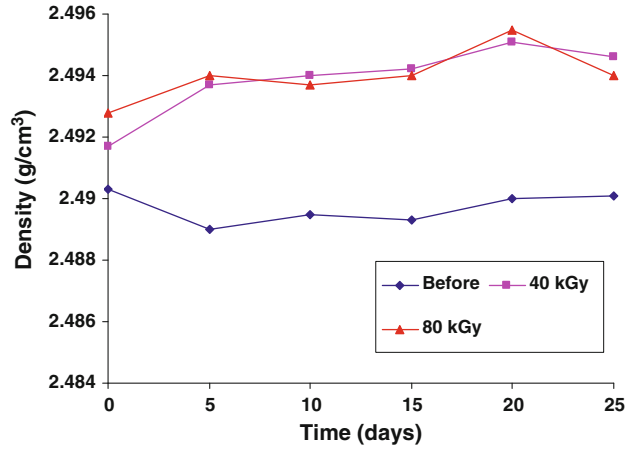

Fig. 18 Effect of different irradiation doses on the density of G1 glass after been immersed in 0.5 N HF at RT

decrease of the glass density by increasing the acid concentration and this can be due to the formation of insoluble CaF_2 and AlF_3 on the glass surface which causes to some extent inhibition of Si ions release.

Irradiation with γ-rays is assumed to be able to create displacements, electronic defects, and/or breaks in the network bonds [43, 44], which allow the structure to reform or compact and fill the relatively large interstices that exist in the interconnected network of silicon and oxygen allowing the formation of different ring configurations such that the average ring size is smaller thus leading to a denser structure causing the observed increase in both density and impact toughness for the unetched glass (G1) and irradiated at 40 kGy (Figs. 17 and 18). As the irradiation progresses (80 kGy) there is a relaxation of the network structure due to the formation of NBO's causing the observed decrease in both density and impact toughness. The sudden drop in impact toughness values for the irradiated glass after been etched may be correlated to the attack of the F^- ions to the Si–O–Si network allowing weakness of the network structure, beside the release of silicon ion to the etchant solution causing the observed increase in density values (Figs. 17 and 18).

Conclusion

The glass used in this study, is a commercial SLS glass, together with two simulated laboratory prepared glasses were investigated for the determination of the effect of the damages generated by different concentrations of HF aqueous solutions at several temperatures and after being irradiated with different irradiation doses.

The commercial SLS glass is found to be more durable than the simulated glasses, which is referred to high compaction of the glass structure due to the presence of Mg^{2+} ions which introduces another compact structure building MgO_4 units.

Several mechanisms of the dissolution reactions are proposed by assuming the adsorption of the two reactive species, namely, HF and HF_2^- and the catalytic action of H^+ ions, and the effect of this adsorption on the siloxane bonds at the glass surface which dominate the dissolution process.

The change in the IR intensity of each spectral band is attributed to the formation or concentration of a given chemical unit. From the results it is concluded that peak at 1050 cm^{-1} represents the combination of Si–O–Si and Si–OH in the glass surface, giving almost the same reflectance even when the glass was etched in 0.5 M HF solution. This peak is observed to shift slowly toward the higher wave number of Si stretching peak due to the formation of $=SiF_2$ and $-SiF_3$ in the glass surface.

During the HF acid treatment of the commercial SLS glass, morphological changes were observed on the surface flaws by SEM. Accordingly, the optical transmission and impact toughness of the treated glasses were affected. At the beginning of the HF etching treatment, a surface deterioration is assumed to be characterized by the opening and the blunting of the surface cracks. This is assumed to cause an improvement in the optical transmission and a decrease of both impact toughness and density. As the etching treatment progresses the disparity between the cracks and the surrounding grooves diminishes resulting into larger and less deep hollows. This is assumed to cause degradation in optical transmission and an improvement of both impact toughness and density.

Also, the results allow concluding that structural transformations caused in the virgin studied SLS glass matrix by irradiation and consequent formation and annihilation of NBO's and changes the chemical bonding in the glass surface which affect the efficiency of glass interaction with hydrofluoric acid solution. It is important to notice that induced-radiation defects precede etching produced

significantly lower durability compared to the conventional chemical etching. Also, irradiation is observed to improve both impact toughness and density while optical transmission degrades than the unirradiated, but even this degradation of the SLS glass maintained their optical properties.

References

1. Doremus RH (1994) Glass science, 2nd edn. Wiley-Interscience, New York
2. Belyustin AA, Schultz MM (1983) Glass Phys Chem 9:3
3. Clark DE, Pantano CG, Hench LL (1979) Corrosion of glass. Books for Industry, NewYork
4. Speirings GACM (1993) J Mat Sci 28:6261
5. Suratwala T, Wong L, Miller PE, Feit MD, Menapace J, Davis P, Steele R (2006) J Non-Cryst Solids 352:5601
6. Kolli M, Hamidouche M, Bouaoudja N, Fantozzi G (2009) J Eur Cer Soc 29:2697
7. Judge J (1971) J Electrochem Soc 118(11):1772
8. Herman Broene H, DeVries T (1947) J Am Cer Soc 69:1644
9. Geotti-Bianchini F, Pero M, Guglielmi M, Pantano CG (2003) J Non-Cryst Solids 321:110
10. Akai T, Kuraoka K, Chen D, Yamamoto Y, Shirakami T, Jrabe K (2005) J Am Cer Soc 88(10):2962
11. Paul A (1982) Chemistry of glasses. Chapman and Hall, New York
12. Robert E, Whittington A, Fayon F, Pichrvant M, Massiot D (2001) J Chem Geol 174:291
13. Xue X, Kanzaki M (2004) Geochim Cosmochim Acta 68:5027
14. Kohn SC, Dupree R, Smith ME (1989) Nature 337:539
15. Ojovan MI, Lee WE (2004) J Nucl Mater 335:425
16. Devine RAB (1994) Nucl Inst Meth Phys Res B 91:378
17. Arrora M, Baccaro S, Sharma G, Singh D, Singh KS, Thind KS, Singh DP (2009) J Nucl Inst Meth Phys Res B 267:817
18. Weber WJ (1988) J Nucl Inst Meth Phys Res B 32:471
19. Weber WJ, Wald JW, McVay GL (1985) J Am Cer Soc 68:C253
20. Vallet-Regi M, Ragel CV, Salinas AJ (2003) J Inorg Chem 42:1029
21. Wong L, Suratwala T, Feit MD, Miller PE, Steele R (2009) J Non-Cryst Solids 355:797
22. Shelby JE, Vitiko Jr, Pantano CG (1980) J Solar Energy Mater 3:97
23. Leed EA, Pantano CG (2003) J Non-Cryst Solids 325:48
24. Carnali JO, Lugo GM, Sharma A, Jain H (2004) J Non Cryst Solids 341:101
25. Friebele EJ (1991) In: Uhlmann DR, Kreidl NJ (eds) Optical properties of glasses. American Ceramic Society, Westerville, Ohio, p 205
26. El-Batal FHA, Ezz-Eldin FM (2007) J Trans Ind Ceram Soc 66(4):175
27. Ismail SA, Ezz-Eldin FM (2004) Glass Tech 45(5):220
28. Watson EB (1994) Rev Min 30:371
29. Jin cheng D, Cormack AN (2005) J Non-Cryst Solids 351:2263
30. MacDonald SA, Schardt CR, Masiello DJ, Simmons JH (2000) J Non-Cryst Solids 275:72
31. Sholze H (1991) Glass: nature, structure and properties, 3rd edn. Springer, New York
32. Clark DE, Dilmore MF, Ethridge EC, Hench LL (1976) J Am Cer Soc 59(1–2):62
33. Lynch ME, Folz DC, Clark DE (2007) J Non-Cryst Solids 353:2667
34. Safi M, Chazalviel JN, Cherkaoui M, Belaidi A, Gorochov O (2002) J Electrochim Acta 47:2573
35. Clark DE, Ethridge EC, Dilmore MF, Hench LL (1977) Glass Technol 18:121
36. Bunker BC, Tallant DR, Headleey TJ, Turner GL, Kirkpatrck RJ (1988) Phys Chem Glasses 29(3):106
37. Elmer TH, Nordberg ME (1988) J Glastech Ber 61(5):140
38. Chinyama GK, Roos A, Karlsson B (1993) J Solar En 50(2):105
39. Benbahouche S, Roumili F, Seghir A, Zegadi R (2006) J Eur Cer Soc 26(9):1673
40. Gunasekera SP, Holloway DG (1973) Phys Chem Glass 14:45
41. Pantano C Jr, Dove DB, Onado GY (1975) J Non-Cryst Solids 19:41
42. Boenish DW, Gislason SR, Oelkers EH, Putnis CV (2004) J Geochim Cosmochim Acta 68(23):4843
43. Ezz-Eldin FM, El-Alaily NA, El-Batal HA (1992) J Radio-Anal Nucl Chem 63(2):267
44. El-Alaily NA, Mohamed RM (2003) J Mat Sci Eng B 98(3):193